

Instability of a liquid film flow over a vibrating inclined plane

By **DAVID R. WOODS AND S. P. LIN**

Department of Mechanical and Aeronautical Engineering, Clarkson University,
Potsdam, NY 13699-5725, USA

(Received 29 August 1994 and in revised form 10 February 1995)

The problem of the onset of instability in a liquid layer flowing down a vibrating inclined plane is formulated. For the solution of the problem, the Fourier components of the disturbance are expanded in Chebychev polynomials with time-dependent coefficients. The reduced system of ordinary differential equations is analysed with the aid of Floquet theory. The interaction of the long gravity waves, the relatively short shear waves and the parametrically resonated Faraday waves occurring in the film flow is studied. Numerical results show that the long gravity waves can be significantly suppressed, but cannot be completely eliminated by use of the externally imposed oscillation on the incline. At small angles of inclination, the short shear waves may be exploited to enhance the Faraday waves. For a given set of relevant flow parameters, there exists a critical amplitude of the plane vibration below which the Faraday wave cannot be generated. At a given amplitude above this critical one, there also exists a cutoff wavenumber above which the Faraday wave cannot be excited. In general the critical amplitude increases, but the cutoff wavenumber decreases, with increasing viscosity. The cutoff wavenumber also decreases with increasing surface tension. The application of the theory to a novel method of film atomization is discussed.

1. Introduction

The linear stability of a liquid layer flowing down an inclined plane was investigated by Benjamin (1957) and Yih (1963). They found that the film flow is very susceptible to the instability caused by gravity-driven long waves. The nonlinear theories of film instability can be found in the review articles by Lin (1983, 1986) and Chang (1994). Lin (1967), DeBruin (1974), Chin, Abernathy & Bertschy (1986), and Floryan, Davis & Kelly (1987) showed that the film instability may also be caused by relatively short shear waves when the angle of inclination is sufficiently small. The former mode of instability occurs at low Reynolds numbers, and the latter mode occurs at much larger Reynolds numbers. The shear waves in a film flow have the same origin as in Poiseuille flow. The former mode has been termed the soft mode and the latter the hard mode.

In many applications, the inclined plane experiences vibration which is introduced either intentionally or unintentionally. The vibration imparted to the plane may parametrically excite the so-called Faraday waves. It may also excite Stokes–Rayleigh waves in the viscous liquid layer. The parametrically resonated interfacial waves between two unbounded fluids was investigated by Jacqmin & Duval (1988). Recent works on the Faraday waves can be found in the review articles by Wu (1994), Craik (1994) and Miles & Henderson (1990). Statistical studies of chaotic Faraday waves have been made by Gluckman, Arnold & Gollub (1995). The consequence of the interaction among the soft and hard modes of disturbances with the periodically

excited waves in a film flow is of considerable theoretical and practical interest. The problem of linear instability of a liquid layer flowing down an inclined plane is formulated in the next section. The solution by use of the spectral method and the Floquet theory is described in §3. Numerical results are presented in §4. The physical significance of the results and a possible application of the theory to a new technology of atomization is discussed in the last section. Atomization is widely used in many industrial applications including fuel spray formation, waste treatment, powder metallurgy, powder milk production, chemical sprays, high-tech surface cleaning, and advanced material processings.

2. Formulation of the problem.

Consider the stability of a Newtonian liquid film flow down an inclined plane making an angle θ with the horizontal, as shown in figure 1. The rigid inclined plane oscillates sinusoidally with a constant frequency Ω . The amplitudes of oscillation in the directions parallel and perpendicular to the plane are respectively given by ξ and ζ . The liquid is assumed to be incompressible, and the effect of the ambient gas is neglected. The governing equations of the liquid motion in a reference frame moving with the inclined plane are

$$\left. \begin{aligned} \partial_t V + V \cdot \nabla V &= \frac{1}{\rho} \nabla P + \nu \nabla^2 V + \mathbf{g} - A(t), \\ \nabla \cdot V &= 0, \end{aligned} \right\} \quad (1)$$

where t is time, V is the velocity vector, ρ is density, P is the pressure, ν is the kinematic viscosity, \mathbf{g} is the gravitational acceleration and $A(t)$ is the acceleration associated with the D'Alembert body force. The Cartesian components of A in the X - and Y -directions are given respectively by

$$A_1(t) = \xi \Omega^2 \sin \Omega t \quad \text{and} \quad A_2(t) = \zeta \Omega^2 \sin \Omega t.$$

Note that the X -axis is fixed at the mid-depth of the unperturbed liquid layer of thickness $2D$. The Cartesian axis Z is perpendicular to the (X, Y) -plane. The boundary conditions corresponding to (1) include the no-slip condition at the inclined plane $Y = -D$, i.e.

$$V(X, -D, Z) = 0. \quad (2)$$

At the free surface $Y = H(X, Z, t)$, the kinematics require

$$V = (\partial_t + V \cdot \nabla) H, \quad (3)$$

where V is the Y -component of $V = (U, V, W)$. Balancing all forces acting on a unit area of the free surface, we have

$$\sigma \cdot \mathbf{n} + \mathbf{n} S \nabla \cdot \mathbf{n} = 0, \quad (4)$$

where S is the surface tension, \mathbf{n} is the unit outward normal vector related to $F = Y - H$ by

$$\mathbf{n} = \nabla F / |\nabla F|, \quad (5)$$

and σ is the stress tensor. For the incompressible Newtonian fluid, σ is given by

$$\sigma = -P\delta + \mu[\nabla V + (\nabla V)^T],$$

where δ is the Kronecker delta, μ is the dynamic viscosity and the superscript T denotes transpose.

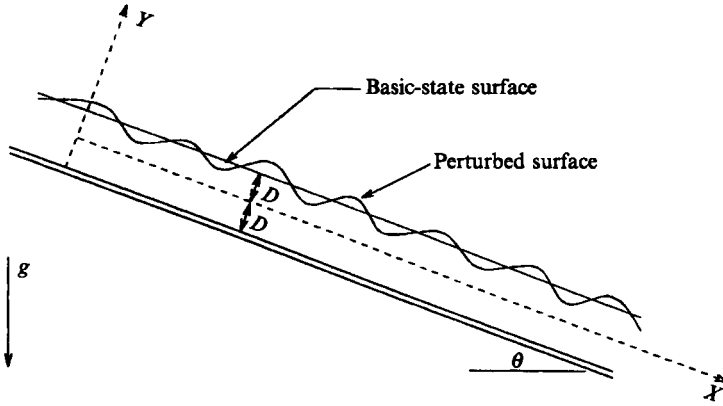


FIGURE 1. Diagram of the theoretical model.

In the dimensionless quantities defined by

$$\begin{aligned} (x, y, z) &= (X, Y, Z)/D, & (d_x, d_y) &= (\xi, \zeta)/D, & h_1 &= H/D, \\ \omega &= \Omega D/E_0 = 1, \\ (u, v, w) &= (U, V, W)/E_0, \\ a &= A/E_0 \Omega, \\ p &= P/\rho E_0^2, & \tau &= tE_0/D, & Re &= DE_0/\nu, \\ Fr &= gD/E_0^2, & Fr &= Fr(\sin \theta, -\cos \theta), & We &= S/\rho E_0^2 D, \end{aligned}$$

(1) and its boundary conditions can be rewritten as

$$(\partial_\tau - v \cdot \nabla) v = -\nabla p + Re^{-1} \nabla^2 v + Fr - a, \tag{6}$$

$$\nabla \cdot v = 0, \tag{7}$$

$$v = 0 \text{ at } y = -1; \tag{8}$$

$$\tau \cdot n + nWe \nabla \cdot n = 0 \text{ at } y = h_1, \tag{9}$$

where $\tau = \sigma/\rho E_0^2$ is the dimensionless stress tensor. It should be pointed out that the gradient operator and the Laplacian in (6)–(9) are now in dimensionless spatial variables (x, y, z) .

It is easily verified that an exact solution of the differential system (5)–(9) is given by

$$\bar{u} \equiv u(y, \tau) = \frac{1}{2} Re Fr \sin \theta (3 + 2y - y^2) + d_x \cos \omega \tau + \bar{u}_0(y, \tau), \tag{10}$$

where

$$\bar{u}_0(y, \tau) = d_x [f_1(\tau) G_1(y) + f_2(\tau) G_2(y)],$$

$$f_1(\tau) = -\cos \omega \tau, \quad f_2(\tau) = \sin \omega \tau,$$

$$G_1(y) = \frac{ac + bd}{c^2 + d^2}, \quad G_2(y) = \frac{bc - ad}{c^2 + d^2},$$

$$\bar{p} \equiv p(y, \tau) = p_0 - [Fr \cos \theta + d_y \sin \omega \tau](y - 1),$$

$$\bar{v} = \bar{w} = 0,$$

where p_0 is a reference pressure, and

$$a = e^{\beta y} \cos \beta y + e^{\beta(2-y)} \cos [\beta(2-y)], \quad b = e^{\beta y} \sin \beta y + e^{\beta(2-y)} \sin [\beta(2-y)],$$

$$c = e^{-\beta} \cos \beta + e^{3\beta} \cos 3\beta, \quad d = -e^{-\beta} \sin \beta + e^{3\beta} \sin 3\beta, \quad \beta = (Re/2)^{1/2}.$$

The exact solution given by (10) represents an unsteady parallel flow with a flat free surface. This is the basic flow the stability of which is being considered.

Here we consider only the onset of instability with respect to two-dimensional disturbances. We perturb the basic flow with disturbances which are represented by primed quantities, and write

$$\left. \begin{aligned} u &= \bar{u} + u'(x, y, \tau), & v &= v', & w' &= 0, \\ p &= \bar{p} + p'(x, y, \tau), & h_1 &= 1 + \eta. \end{aligned} \right\} \tag{11}$$

In terms of the Stokes stream function, the velocity disturbance can be written as

$$u' = \psi_y, \quad v' = -\psi_x, \tag{12}$$

where the subscripts denote partial differentiation. We seek a normal-mode solution of the form

$$(\psi, p', \eta) = [\phi(y, \tau), f(y, \tau), h(\tau)] e^{i\alpha x}, \tag{13}$$

where α is the wavenumber, and ϕ, f , and h are the amplitude functions of ψ, p' and η respectively. Substituting (12) and (13) into the curl of (6) and neglecting the nonlinear terms, one obtains the partial differential equation for ϕ :

$$Re[(\partial_\tau + i\alpha\bar{u})(\phi_{yy} - \alpha^2\phi) - i\alpha\bar{u}_{yy}\phi] - \phi_{yyy} + 2\alpha^2\phi_{yy} - \alpha^4\phi = 0. \tag{14}$$

This is the well known Orr–Sommerfeld equation (Orr 1907; Sommerfeld 1908) except that ϕ here is an implicit function of time as well as y . Hence the partial time-derivative term that appears in (14) takes the place of the $i\alpha$ -term arising from time differentiation in the original Orr–Sommerfeld equation for steady basic flow. The primes in (14) denotes differentiation with respect to y . Substituting (11) into (8) and (9), expanding u' and p' in Taylor's series about $y = 1$, and neglecting nonlinear terms, one has the boundary conditions at $y = 1$:

$$v' = (\partial_\tau + \bar{u}\partial_x)\eta, \tag{15}$$

$$\eta\partial_{yy}\bar{u} + \partial_y u' + \partial_x v' = 0, \tag{16}$$

$$\eta\partial_y\bar{p} + p' - \frac{2}{Re}\partial_y v' + We\partial_{xx}\eta = 0, \tag{17}$$

where p' is found from (6) with a linear approximation to be

$$p' = \frac{1}{i\alpha} \left[\frac{1}{Re}(\partial_{xx}u' + \partial_{yy}u') - \bar{u}\partial_x u' - \partial_\tau u' \right]. \tag{18}$$

Note that (16) and (17) arise from the tangential and normal components of (9), respectively. Substituting (10), (12) and (13) into (8) and (15)–(17), one has

$$\phi(-1, \tau) = \phi'(-1, \tau) = 0, \tag{19}$$

$$[\partial_\tau + i\alpha\bar{u}(1, \tau)]h + i\alpha\phi(1, \tau) = 0, \tag{20}$$

$$\bar{u}''h + \phi''(1, \tau) + \alpha^2\phi(1, \tau) = 0, \tag{21}$$

$$(\partial_\tau + i\alpha\bar{u})\phi'(1, \tau) - \frac{1}{Re}[\phi'''(1, \tau) - 3\alpha^2\phi'(1, \tau)] + i\alpha[Fr \cos \theta + d_y \sin \omega\tau + \alpha^2 We]h = 0. \tag{22}$$

The differential system consisting of (14) and (19)–(22) is to be solved to determine the condition of stability for the basic flow described in (10).

3. Chebyshev–Floquet solution

The solution of (14) will be constructed as a finite sum of the Chebyshev polynomials,

$$\phi(y, \tau) = \sum_{n=0}^N a_n(\tau) T_n(y),$$

where N is an integer yet to be determined, $T_n(y)$ is the n th Chebyshev polynomial defined by

$$T_n(y) = \cos(n \cos^{-1} y), \quad -1 \leq y \leq 1,$$

and $a_n(\tau)$ is an unknown function of time. There are terms in (14) which are products of powers of y and the derivatives in y of ϕ . It can be shown that (Gottlieb & Orszag 1986) these terms can be expanded as

$$y^r \phi^{(q)}(y, \tau) = \sum_{n=0} b_n(\tau) T_n(y), \tag{23}$$

where b_n are related to a_n for any given power r and the q th-order derivative. For example, the $b_n(\tau)$ for $r = 0, q = 2$ in (23) is

$$c_n b_n(\tau) = \sum_{\substack{p=n+p \\ n+p=\text{even}}} p(p^2 - n^2) a_p(\tau), \tag{24}$$

and $b_n(\tau)$ in the expansion of $y\phi''$ is related to $a_n(\tau)$ by

$$c_n b_n = 2n(n+1) a_{n+1} + \sum_{\substack{p=n+3 \\ n+p=\text{odd}}} p(p^2 - n^2 - 1) a_p,$$

where $c_n = 0$ if $n < 0$, and $c_0 = 2, c_n = 1$ when $n > 0$.

The terms involving exponential functions in (14) can also be expanded in the Chebyshev series. First, u_0 and u_0'' can be expanded as

$$\left. \begin{aligned} \bar{u}_0 &= d_x [f_1(\tau) \sum_{n=0} k_{1n} T_n(y) + f_2(\tau) \sum_{n=0} k_{2n} T_n(y)] \\ \bar{u}_0'' &= d_x [f_1(\tau) \sum_{n=0} k_{3n} T_n(y) + f_2(\tau) \sum_{n=0} k_{4n} T_n(y)]. \end{aligned} \right\} \tag{25}$$

$k_{in} (i = 1, 2, 3, 4)$ in (25) can be found by use of the orthogonal property of the Chebychev polynomials,

$$k_{in} = \frac{2}{\pi c_n} \int_{-1}^1 G_i(y) (1 - y^2)^{1/2} T_n(y) dy, \quad i = 1, 2, 3, 4,$$

where G_1 and G_2 are defined following (10), and

$$G_3(y) = G_1'(y), \quad G_4(y) = G_2''(y).$$

It can be shown that

$$\sum_{n=0} a_n(\tau) T_n(y) \sum_{m=0} k_{im} T_m(y) = \sum_{n=0} e_{in}(\tau) T_n(y), \tag{26}$$

where

$$c_n e_{in}(\tau) = \frac{1}{2} \sum_{m=-\infty}^{\infty} \bar{a}_{n-m}(\tau) \bar{k}_{im},$$

$$\bar{a}_n = c_{|n|} a_{|n|}, \quad \bar{k}_{|n|} = c_{|n|} k_{i|n|}.$$

It follows from (25) and (26) that

$$(\bar{u}_0 \phi, \bar{u}'_0 \phi) = d_x \sum_{i=1} \left[\left(\sum_{i=1}^2 f_i, \sum_{i=3}^4 f_{i-2} \right) \frac{1}{2c_n} \sum_{\substack{|p|-N \\ |n+p| \leq N}} \bar{a}_p(\tau) \bar{k}_{i(n-p)} \right] T_n(y).$$

It follows from (24), (25) and (26) that

$$\bar{u}_0 \phi'' = d_x \sum_{n=0} \left[\sum_{i=1}^2 f_i \frac{1}{2c_n} \sum_{\substack{p=2 \\ |n-m| \leq N \\ |m| \leq p-2}} a_p(\tau) \sum_{\substack{p(p^2-m^2) \\ |n-m| \leq N \\ |m| \leq p-2}} \bar{k}_{i(n-m)} \right] T_n(y),$$

where $(m+p)$ is even. Substituting all relevant expansions into (14) and demanding the coefficient of $T_n(y)$ to be zero for $n = 0$ to N , one has

$$\begin{aligned} & -\frac{1}{24} \sum_{\substack{p=n+4 \\ n+p \text{ even}}}^N [p^3(p^2-4)^2 - 3n^2p^5 + 3n^4p^3 - n^2(n^2-4)p] a_p(\tau) \\ & + i\alpha Q \sum_{\substack{p=n+3 \\ n+p \text{ odd}}}^N p(p^2-n^2-1) a_p(\tau) + \sum_{\substack{p=n+2 \\ n+p \text{ even}}}^N [2\alpha^2 - \frac{1}{2}i\alpha Q p(p^2-n^2-2) \\ & + \frac{3}{2}i\alpha Q + i\alpha Re d_x \cos \omega\tau] a_p(\tau) + [-\alpha^4 + \frac{1}{8}i\alpha^3 Q(c_n - c_{n-1}) - i\alpha^3(\frac{3}{8}Q + Re d_x \cos \omega\tau) \\ & + i\alpha Q - \frac{1}{2c_n} i\alpha Q n(n-1)] c_n a_n(\tau) + \frac{1}{8}i\alpha^3 Q c_{n-2} c_n a_{n-2}(\tau) \\ & - \frac{1}{2}i\alpha^3 c_n c_{n-1} a_{n-1}(\tau) + i\alpha Q [2n(n+1) - \frac{1}{2}\alpha^2 c_n] a_{n+1}(\tau) \\ & + \frac{1}{8}i\alpha^3 Q c_n a_{n+2}(\tau) - i\alpha^3 Re d_x \sum_{i=1}^2 f_i(\omega\tau) \frac{1}{2} \sum_{\substack{|p| \leq N \\ |n+p| \leq N}} \bar{a}_p(\tau) \bar{k}_{i(n-p)} \\ & + i\alpha Re d_x \sum_{i=1}^2 f_i(\omega\tau) \frac{1}{2} \sum_{p=2}^N a_p(\tau) \sum_{\substack{|n-m| \leq N \\ |m| \leq p-2}} p(p^2-m^2) \bar{k}_{i(n-m)} \\ & - i\alpha Re d_x \sum_{i=3}^4 f_{i-2}(\omega\tau) \sum_{\substack{|p| \leq N \\ |n+p| \leq N}} \bar{a}_p(\tau) \bar{k}_{i(n-p)} \\ & = -Re \sum_{\substack{p=n+2 \\ n+p \text{ even}}}^{\infty} p(p^2-n^2) \dot{a}_p(\tau) + \alpha^2 Re c_n \dot{a}_n(\tau). \end{aligned} \tag{27}$$

Substituting the Chebyshev expansion of ϕ into the boundary conditions (19)–(22), and using the relations $T_n(-1) = (-1)^n$, $T'_n(-1) = (-1)^{n+1}$, $T_n(1) = 1$, $T'_n(1) = n^2$, $T''_n(1) = n^2(n^2-1)/3$, $T'''_n(1) = n^2(n^2-1)(n^2-4)/15$, we have

$$\sum_{n=0}^N (-1)^n a_n = 0, \tag{28}$$

$$\sum_{n=0}^N (-1)^{n-1} a_n = 0, \tag{29}$$

$$i\alpha \sum_{n=0}^N a_n + i\alpha \bar{u}(1, \tau) h + \dot{h} = 0, \tag{30}$$

$$\sum_{n=0}^N [\alpha^2 + \frac{1}{3}n^2(n^2-1)] a_n + \bar{u}''(1, \tau) h = 0, \tag{31}$$

$$\sum_{n=0}^N n \dot{a}_n + \sum_{n=0}^N \frac{n^2}{Re} [i\alpha \bar{u}(1, \tau) Re + 3\alpha^2 - \frac{1}{15}(n^2-1)(n^2-4)] a_n + i\alpha [Fr \cos \theta + dy \sin \omega t + \alpha^2 We] h = 0. \tag{32}$$

The Chebyshev expansion solution has reduced the problem to a system of ordinary differential equations in time with $N+2$ unknowns: a_0, a_1, \dots, a_N and h . Five of the required $(N+2)$ equations are supplied by the boundary conditions (28)–(32). The other $(N-3)$ equations are obtained from (27) with $n = 0, 1, \dots, N-4$. This is the so-called Lanzo’s method of approximation (Orszag 1971).

The system (27)–(32) can be summarized as

$$\mathbf{A}(\tau) \mathbf{x} = \mathbf{B} \dot{\mathbf{x}} \tag{33}$$

where $\mathbf{x} = (a_0, a_1, \dots, a_N, h)$, \mathbf{A} is a continuous 2π -periodic matrix and \mathbf{B} is a constant matrix whose elements can be read off from (27)–(32). According to the Floquet theory (see e.g. Nayfeh & Mook 1979), there exists a constant matrix \mathbf{R} such that for all τ ,

$$\mathbf{S}(\tau + T) = \mathbf{R} \mathbf{S}(\tau), \tag{34}$$

where T is the period, i.e. 2π , and \mathbf{S} is the fundamental solution matrix satisfying

$$\mathbf{A}(\tau) \mathbf{S} = \mathbf{B} \dot{\mathbf{S}}. \tag{35}$$

Moreover, if the characteristic roots of \mathbf{R} are $\lambda_i (i = 1, 2, \dots, m)$, then the solution of (33) can be written as

$$x_i = e^{\gamma_i \tau} z_i(\tau) \quad \text{with} \quad z_i(\tau + T) = z_i(\tau), \tag{36}$$

where the characteristic exponents γ_i are related to the characteristic roots by

$$\gamma_i = \frac{1}{T} \ln \lambda_i. \tag{37}$$

Thus, to find γ_i one must first find \mathbf{R} . It is seen from (34) that

$$\mathbf{S}(T) = \mathbf{R} \mathbf{S}(0).$$

Therefore \mathbf{R} can be obtained by integrating (35) over one period with $\mathbf{S}(0) = \mathbf{I}$, where \mathbf{I} is the identity matrix. The stability property is determined by the sign of γ_i . The basic flow is linearly stable if the real part of γ_i is positive, if it is negative the flow is stable.

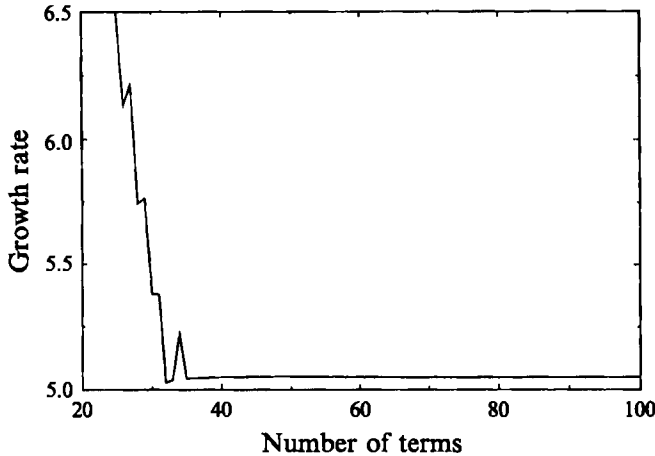


FIGURE 2. Convergence test: $Re = 600$, $We = 0.008$, $Fr = 0.001$, $\theta = 30^\circ$.

Otherwise the flow is neutrally stable. The imaginary part of γ_i determines the frequency response of the perturbed flow to the 2π -periodic forcing. The dimensionless forcing frequency is $2\pi/T = 1$. It follows from (36) and (37) that the frequency of the disturbance is shifted from 1 by an amount

$$(\gamma_i)_i = \frac{1}{2\pi} \{ \tan^{-1} [(\lambda_i)_i / (\lambda_i)_r] + 2k\pi \},$$

where $(\lambda_i)_i$ and $(\lambda_i)_r$ are respectively the imaginary and real parts of λ_i , and k is any integer.

The integration of (35) over one forcing period to obtain \mathcal{R} was achieved by use of a sixth-order Runge–Kutta scheme from the IMSL software library. A less accurate but faster method by Hsu (1974) was used to spot check the results obtained with the Runge–Kutta method. The eigenvalues of \mathcal{R} were obtained by use of the software DEVCCG of the IMSL library. Several measures were taken to check the possible syntax and program errors. It is known (Lin 1967; DeBruin 1974) that the present problem with $d_x = d_y = 0$, $\theta = 90^\circ$, and $We = 0$ reduces to that of plane Poiseuille flow. With these parameter values, the results obtained by Orszag (1971) for plane Poiseuille flow were recovered. For the case of $\theta = 0$, the eigenvalues were also obtained by expanding $z(\tau)$ in (36) in Fourier series. The eigenvalue γ thus obtained is compared with that obtained from (37). Good agreement was found for various flow parameters. The number of terms required in the Chebyshev series representation was determined by successively increasing N until further increase in N resulting in no further improvement in accuracy. At least three-decimal-point accuracy is achieved in all of the results to be reported. The minimum value of N required depends on flow parameters. It is most sensitive to the change in Re . A typical convergence test is displayed in figure 2.

Although the formulation of the problem and the method of solution allow consideration of both the Faraday and the Stokes–Rayleigh waves, we have obtained only the results for the case of plane oscillation perpendicular to the incline. Therefore in the results to be presented in the next section $d_x = 0$.

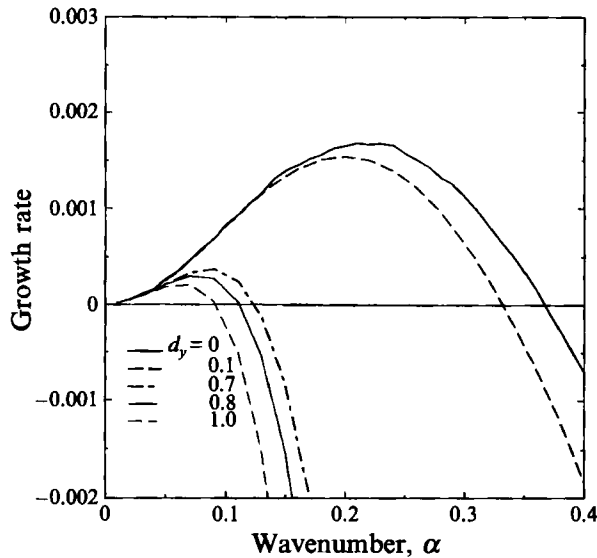


FIGURE 3. Suppression of surface waves: $Re = 5$, $We = 0.016$, $Fr = 0.01$, $\theta = 90^\circ$.

4. Results

Figure 3 shows how the growth rate of the soft-mode long-wave disturbance in an unforced liquid film flow with $d_y = 0$ can be reduced by external forcing of increasing amplitude for the flow parameters listed in the figure caption. However, it is not possible to suppress the long waves completely, because no forcing can be tuned to the frequency of the extremely long waves as will be seen shortly. Figure 4 depicts the neutral curve in the (d_y, α) -plane for the same flow parameters as in figure 3. It shows the ranges of the forcing amplitude which must be used to resonate the disturbance at the subharmonic, synchronous or higher harmonics of the forcing frequencies, for a given α . It should be pointed out that the subharmonic excitation refers to the subharmonic in frequency, it does not refer to the subharmonic in wavenumber. In the unstable region near the origin, the disturbance is untuned to the forcing, and the instability is essentially gravitational. It is seen that for a given forcing amplitude, only disturbances of a certain finite range of wavelength can be excited. Moreover, there is a cutoff wavenumber beyond which the oscillating film is stable. For example, at $d_y = 1$ and 3, only the subharmonic can be excited, but at $d_y = 5$ and 6 both the subharmonic and synchronous waves can be excited. The growth rates corresponding to these values of d_y are plotted in figure 5. Note that growth rate of the synchronous wave is higher than that of the subharmonic one when both exist for the parameters given. However, the subharmonics can be excited more easily with a smaller d_y .

Figure 6 shows the effect of Re on the stability. The critical d_y for each mode of resonant wave is seen to decrease when Re is increased for a given α . Thus in order to produce parametric resonance in a film at a lower forcing amplitude but the same frequency, one may reduce the viscosity of the liquid film of a given thickness and surface tension. The effects of Re on the growth rate are depicted in figure 7. For $Re = 5$ and 10, only the subharmonic resonance can be generated. At $Re = 47.4$ both the subharmonic and the synchronous waves are generated. An additional mode corresponding to the 3/2-mode appears when $Re = 100$ or 150. Contrary to the situation in figure 5, the maximum growth rate of the subharmonic waves is now higher

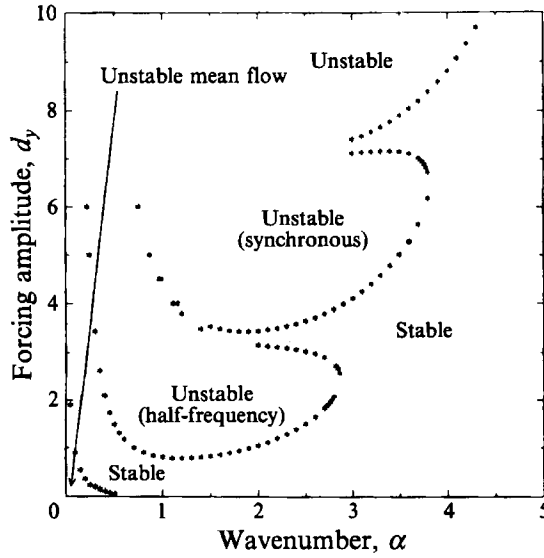


FIGURE 4. Typical neutral curves for the combined flow: $Re = 5$, $We = 0.016$, $Fr = 0.01$, $\theta = 90^\circ$.

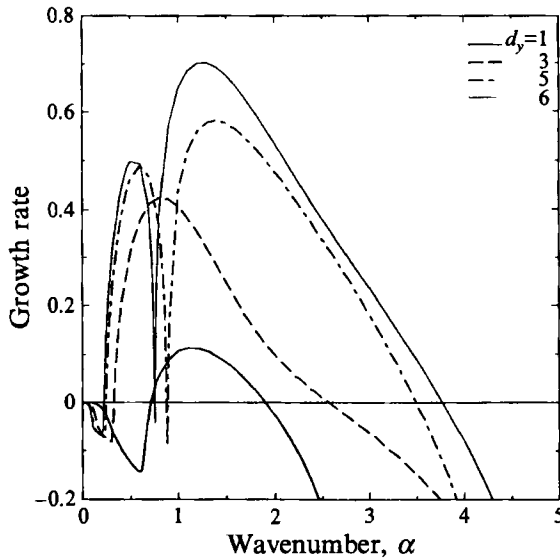


FIGURE 5. Effect of d_y on growth rate: $Re = 5$, $We = 0.016$, $Fr = 0.01$, $\theta = 90^\circ$.

than that for the synchronous waves for $Re = 47.4$ and 100 . Note that while the maximum growth rate of the synchronous waves increases monotonically with Re , in this figure, that of the subharmonics does not change monotonically with Re .

Figure 8 displays the effect of We on the neutral stability curves. It is seen that as We is increased, the neutral curves changes little when α is relatively small. However, the change is drastic when α is relatively large. Both the critical amplitude of instability and the cutoff wavenumber for stability are decreased, as We is increased. The surface tension is only effective in suppressing the waves of wavenumber greater than that determined by the intersection of the lower branch of neutral curves of each mode for different We . For waves of smaller wavenumber, surface tension is actually

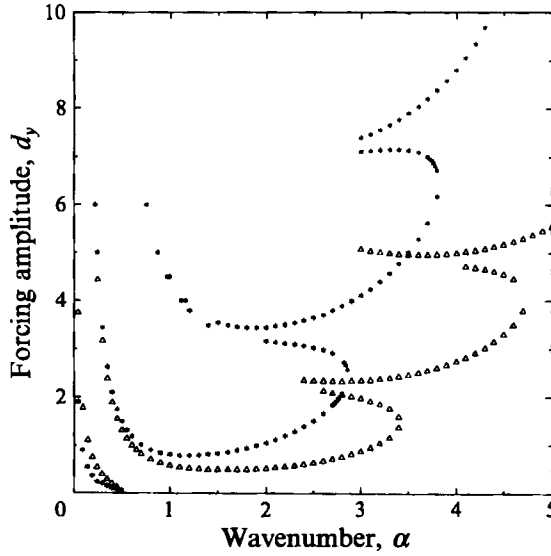


FIGURE 6. Effect of Reynolds number on neutral curves: $We = 0.016$, $Fr = 0.01$, $\theta = 90^\circ$.
*, $Re = 5$; Δ , $Re = 10$.

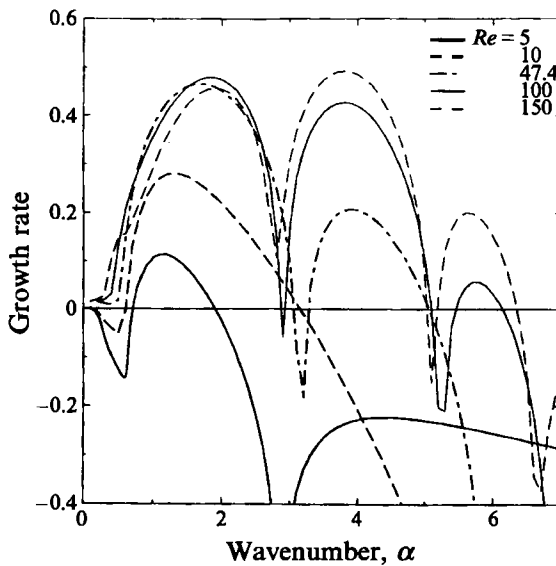


FIGURE 7. Effect of Reynolds number on growth rate: $d_y = 1$, $We = 0.016$, $Fr = 0.01$, $\theta = 90^\circ$.

destabilizing. The suppression of both the subharmonic and synchronous waves by surface tension is depicted in figure 9.

Figure 10 shows that gravity has very little effect on the growth rate of subharmonically resonated waves. In a weightless environment the resonated subharmonic waves are slightly shorter than those observed on Earth for the flow parameters given in the figure caption.

Figure 11 shows that there is no discernible difference in the amplification curves for $\theta = 0^\circ$ and 90° for the parametrically excited waves at the given parameter values. Of course the angle of inclination θ does have a known effect on the amplification of the

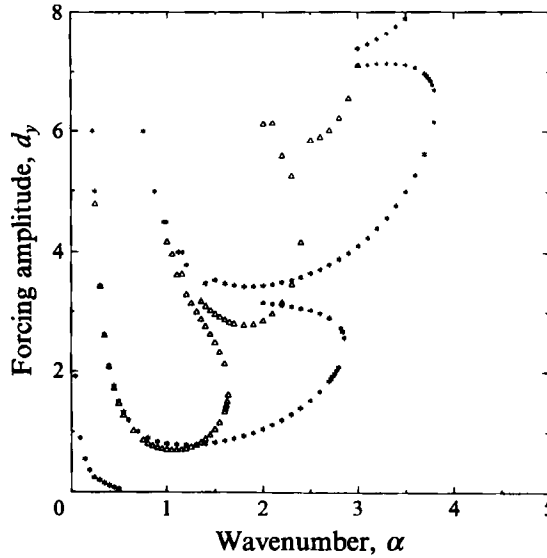


FIGURE 8. Effect of Weber number on neutral curves: $Re = 5$, $Fr = 0.01$, $\theta = 90^\circ$.
 *, $We = 0.016$; Δ , $We = 0.16$.

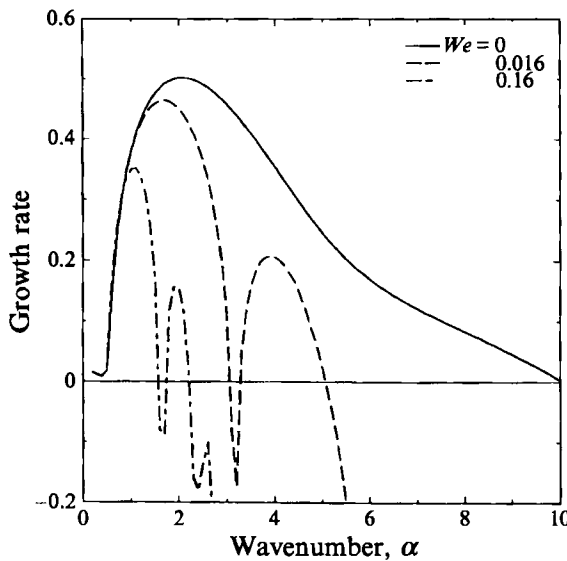


FIGURE 9. Effect of Weber number on growth rate: $d_y = 1$, $Re = 47.4$, $Fr = 0.01$, $\theta = 90^\circ$.

untuned gravity waves near $\alpha = 0$. However, the growth rates of tuned and untuned waves are several orders of magnitude different. Information on the wave speed of stable and unstable disturbances is given in figure 12 for the flow parameters indicated in the figure. The case of $d_y = 0$ is for the unforced film and $d_y = 5$ is for the vibrating film. For the unforced film the appropriate velocity scale is not ΩD . If the average velocity, u_a in the film flow is used as the reference velocity, the Reynolds number Re_y , the Weber number We_y and the Froude number Fr_y for the free film flow can be defined as

$$Re_y = u_a D / \nu, \quad We_y = S / \rho u_a^2 D, \quad Fr_y = g D / u_a^2, \quad u_a = 4gD^2 \sin \theta / 3\nu.$$

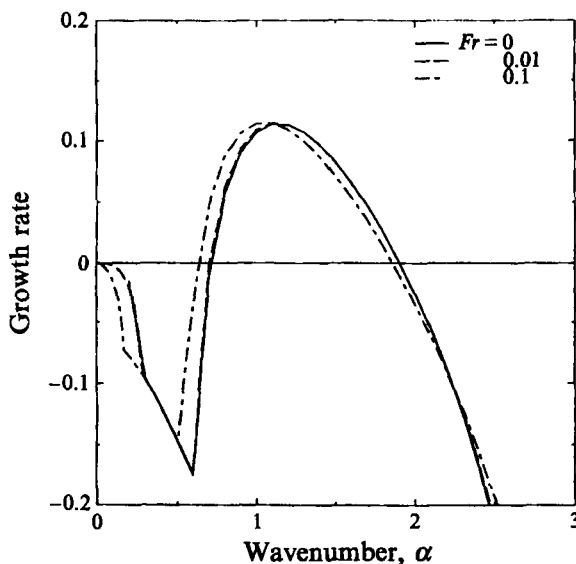


FIGURE 10. Effect of Froude number on growth rate: $d_y = 1$, $Re = 5$, $We = 0.016$, $\theta = 0^\circ$.

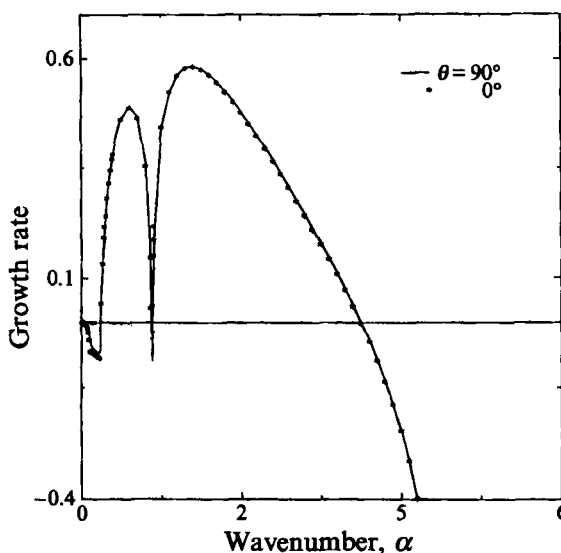


FIGURE 11. Effect of inclination angle on growth rate: $d_y = 1$, $Re = 5$, $We = 0.016$, $Fr = 0.01$.

It can be verified easily that for all Ω ,

$$Re_y = \frac{4}{3} Re^2 Fr \sin \theta, \quad We_y = \frac{9 We}{16 Re^2 Fr^2 \sin^3 \theta}, \quad Fr_y = \frac{3}{Ry^4} \sin \theta.$$

Thus the values of Re_y , We_y and Fr_y corresponding to Re , We and Fr given in the figure caption can be calculated from these equations. It follows from (13) and (36) that the wave speed \bar{c} can be obtained from

$$\bar{c} = -\partial(\gamma_i)_i / \partial \alpha.$$

For the case of $d_y = 5$, the slope of the $(\gamma_i)_i - \alpha$ curve is found to be -0.1 for the tuned stable or unstable waves. Thus \bar{c} is 0.1 , which happens to be equal to $2FrRe$. It is seen from (10) that this is equal to the unperturbed free surface velocity. Therefore the

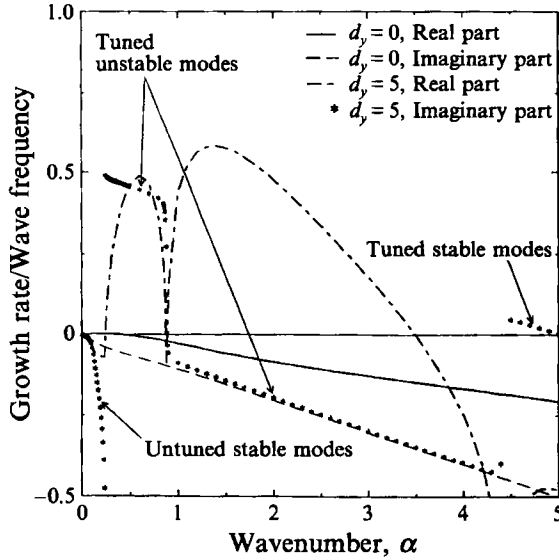


FIGURE 12. Growth rate and wave frequency: $Re = 5$, $We = 0.016$, $Fr = 0.01$, $\theta = 90^\circ$.

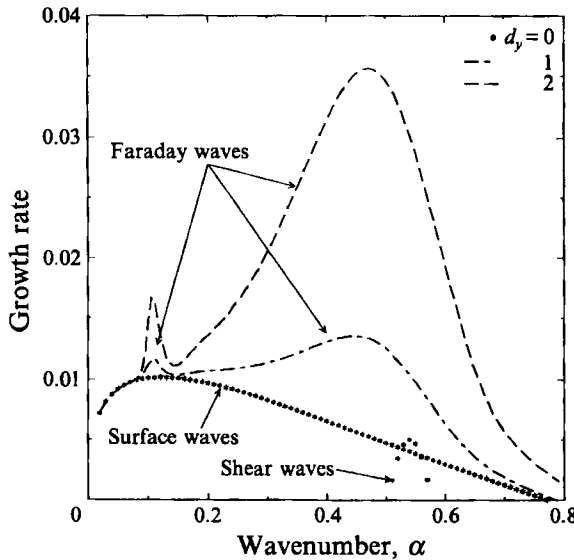


FIGURE 13. The three forms of instability: $Re = 293$, $We = 5$, $Fr = 1$, $\theta = 1^\circ$.

resonated waves are standing waves relative to the moving free surface. However, the untuned stable waves with $\alpha < 0.25$ are highly dispersive, since the slope along the α , $(\gamma_i)_i$ curve is a function of the wavelength. The real and imaginary parts of (γ_i) for the unforced film flow are also given in figure 12 for reference. It is seen that the relatively short stable waves propagate at the free surface velocity in an unforced liquid layer. For relatively long unstable waves the wave speed increases as $\alpha \rightarrow 0$ and approaches 0.2, which is twice the free surface velocity. The jumps in the wave speeds in figure 12 are due to the transition from one domain to another of the excited modes.

At small angle of inclination, one expects to see the emergence of the shear waves (Lin 1967; DeBruin 1974; Chin *et al.* 1986; Floryan *et al.* 1987). Figure 13 shows the

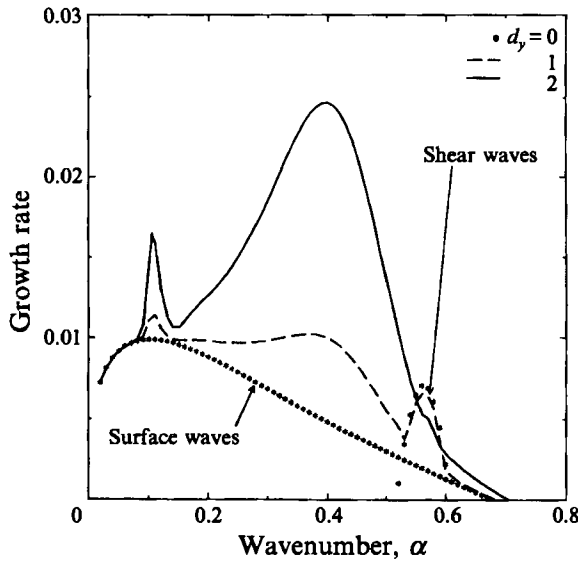


FIGURE 14. Effect of Weber number on shear mode: $We = 10$, other parameters as figure 13.

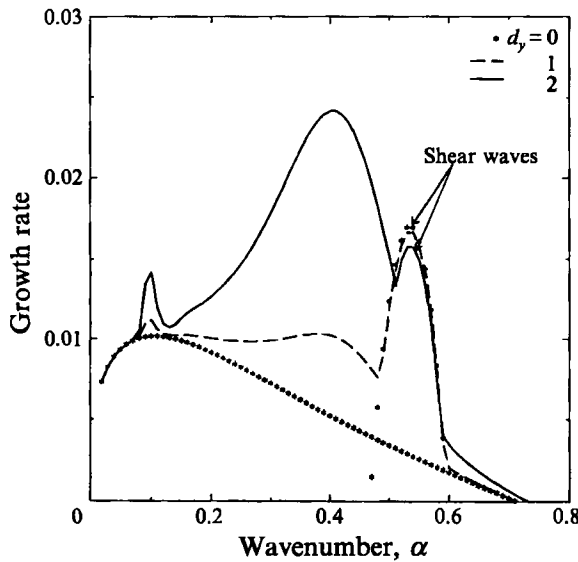


FIGURE 15. Effect of Reynolds number on shear mode: $Re = 327.8$, other parameters as figure 14.

relative magnitudes of the amplification rates for the surface waves, the shear waves and the Faraday waves at the flow parameters given. It is seen that both the surface waves and shear waves are quickly dominated by the Faraday waves as d_y is increased. When the free surface is stiffened by doubling We with the rest of parameters in figure 13 kept constant, the shear waves start to enhance the resonated waves of relatively short wavelength as can be seen in figure 14. When the Reynolds number is increased from that given in figure 14 with the rest of the parameters kept constant, the enhancement of Faraday waves by shear waves becomes very prominent at $d_y = 1$ as shown in figure 15. The maximum amplification rate of the shear waves is actually much larger than the synchronous Faraday waves at $d_y = 1$.

5. Discussion

Three linearly independent wave modes are identified at the onset of instability of a liquid layer flowing down an oscillating inclined plane. The most persistent, though the weakest waves, are the long waves. The growth rate of the unstable long waves may be considerably reduced and their wavelength increased by introducing vibration perpendicular to the incline. However, increasingly large amplitude of vibration must be applied to increase the cutoff wavelength of unstable long waves. It is shown that there exists a critical amplitude of vibration below which the Faraday resonant wave cannot be generated, for a given set of relevant flow parameters. There also exists a critical vibration amplitude below which only the waves which are the subharmonic of the external periodic forcing can be parametrically resonated. Above this second critical amplitude, the subharmonic as well as the higher harmonic waves can be simultaneously resonated. There also exists a cutoff wavelength below which a given forcing is not able to overcome the surface tension to resonate the system. The cutoff wavelength increases with We . On the other hand, the critical amplitude decreases with increasing Re . The growth rate of the subharmonic wave may or may not be greater than the synchronous or higher harmonic waves, depending on the flow parameters.

It is known (Lin 1967; DeBruin 1974; Chin *et al.* 1986; Floryan *et al.* 1987) that at small angles of inclination the relatively short shear waves may emerge at sufficiently large Reynolds numbers to compete with the long gravity wave when the incline is stationary. It is shown that the shear wave may be employed to enhance the growth of the Faraday wave. Although the growth rate of shear waves at small θ may be larger than that of the Faraday waves for a narrow range of wavelength, the former are found to stabilize at larger cutoff wavelengths than that for the Faraday waves as can be seen from figures 14 and 15. Hence the neutral curves delineating the effect of Re , We and Fr on short shear waves at small θ remain qualitatively the same as those depicted in figures 4, 6 and 8. Moreover the excited subharmonics are essentially Faraday waves of wavelength much longer than that of shear waves. Therefore the effects of all relevant parameters in the case of small θ and large Re , for which shear waves may emerge to compete with short Faraday waves, remain qualitatively the same as those depicted in figures 2–12. However, numerical calculation requires much more computer time for Re of order several thousands. It should be pointed out that the shortest waves in a film flow forced at a given set of flow parameters are associated with the Faraday waves, not with the shear waves. The present analysis may be extended to treat three-dimensional disturbances. The fundamental mechanism of instability will probably remain the same. The neglected Stokes–Rayleigh waves associated with $d_x \neq 0$ are expected to have a very weak effect on the resonant Faraday waves. This remains to be demonstrated, however.

The results presented here indicate that a vibrating plate may be used to economically atomize the liquid film flowing over it. Atomization is usually achieved by breaking up a liquid jet into small droplets. A plane liquid film may be made to provide a much larger surface area for a much higher rate of atomization. The produced droplet diameters are controlled by the wavelength of the resonated waves. Thus the atomized droplets will not be of uniform diameter, since the unstable waves have a finite bandwidth of wavelength. If the population of the produced droplets is proportional to the growth rate of the disturbance (Taylor 1940), then the atomized droplets may have a mono- or bi-modal size distribution depending on whether the film is resonated to produce only the subharmonic or both the subharmonic and the synchronous disturbances. One may also produce smaller droplets by reducing the film thickness.

The experiment on atomization is in progress and results will be reported upon completion. Of course, for actual industrial applications, quantitative effects of domain boundary and nonlinearity must be considered. Edge effects on the Faraday waves are discussed by Douady (1990). A nonlinear stability theory of liquid film flow over a vibrating plane will be pursued in future work. In particular the nonlinear interaction between the long subharmonic nonlinear waves (Chang 1994) and the linear subharmonic Faraday waves is of considerable interest. The random self-modulation and spatio-temporal chaos associated with parametric excitation examined by Ezerskii, Kortin & Rabinovich (1986), Ezerskii *et al.* (1986*b*), and Gluckman *et al.* (1994), may also occur in this film flow. The control of the sideband instability of both the soft and hard modes of film waves may be possible.

This work was supported in part by grant no. DAAL03-89-K-0179 and DAAH04-93-G0395, ARO and no. NAG3-1402 of NASA. The computation was carried out with the computer facilities at Clarkson University.

REFERENCES

- BENJAMIN, T. B. 1957 *J. Fluid Mech.* **2**, 554.
 CHANG, H. C. 1994 *Ann. Rev. Fluid Mech.* **26**, 103.
 CHIN, R. W., ABERNATHY, F. H. & BERTSCHY, J. R. 1986 *J. Fluid Mech.* **168**, 501.
 CRAIK, A. 1994 In *Nonlinear Instability of Nonparallel Flows, IUTAM Symp.* (ed. S. P. Lin, W. R. Phillips & D. T. Valentine), p. 374.
 DEBRUIN, G. J. 1974 *J. Engng Maths* **8**, 259.
 DOUADY, S. 1990 *J. Fluid Mech.* **221**, 383.
 EZERSKII, A. B., KORTIN, P. I. & RABINOVICH, M. I. 1986*a* *Sov. Phys. JETP* **41**, 157.
 EZERSKII, A. B., RABINOVICH, M. I., REUTOV, V. P. & STROBINETS, I. M. 1986*b* *Sov. Phys. JETP* **64**, 1228.
 FLORYAN, J. M., DAVIS, S. H. & KELLY, R. E. 1987 *Phys. Fluids* **30**, 983.
 GLUCKMAN, B. J., ARNOLD, C. B. & GOLLUB, J. P. 1995 *Phys. Rev.* (to appear).
 GOTTLIEB, D. & ORSZAG, S. A. 1986 *Numerical Analysis of Spectral Methods*. SIAM.
 HSU, C. S. 1974 *J. Math. Anal. Appl.* **45**, 234.
 JACQMIN, D. & DUVAL, W. M. B. 1988 *J. Fluid Mech.* **196**, 496.
 LIN, S. P. 1983 In *Waves on Fluid Interfaces* (ed. R. E. Meyer), p. 261. Academic.
 LIN, S. P. & WANG, C. Y. 1986 In *Encyclopedia of Fluid Mechanics*, Vol 1 (ed. N. P. Cheremisinoff), p. 931. Gulf.
 LIN, S. P. 1967 *Phys. Fluids* **60**, 308.
 MILES, J. W. & HENDERSON, D. 1990 *Ann. Rev. Fluid Mech.* **22**, 143.
 NAYFEH, A. H. & MOOK, D. 1979 In *Nonlinear Oscillation*, pp. 276–296. John Wiley.
 ORSZAG, S. A. 1971 *J. Fluid Mech.* **50**, 689.
 ORR, W. MCF. 1907 *Proc. R. Irish Acad.* **A27**, 69.
 SOMMERFELD, A. 1908 *Proc. 4th Intl Congr. Math. Rome*, p. 116.
 TAYLOR, G. I. 1940 Generation of ripples by wind blowing over a viscous fluid. Paper written for the Chemical Defence Research Department, Ministry of Science. (Reprinted in *The Scientific Papers of Sir Geoffrey Ingram Taylor*, vol. 3, p. 244, Cambridge University Press, 1940.)
 WU, T. Y. 1994 In *Nonlinear Instability of Nonparallel Flows, IUTAM Symp.* (ed. S. P. Lin, W. R. Phillips & D. T. Valentine), p. 397.
 YIH, C. S. 1963 *Phys. Fluids* **6**, 321.